THE JOURNAL OF CHEMICAL PHYSICS **122**, 044305 (2005)

Ab initio calculations, potential representation and vibrational dynamics of He_2Br_2 van der Waals complex

Álvaro Valdés, Rita Prosmiti,[a] Pablo Villarreal, and Gerardo Delgado-Barrio
Instituto de Matemáticas y Física Fundamental, C.S.I.C., Serrano 123, 28006 Madrid, Spain

(Received 15 September 2004; accepted 25 October 2004; published online 5 January 2005)

An intermolecular potential energy surface for He_2Br_2 complex in the ground state is calculated at the levels of fourth-order (MP4) Møller–Plesset and coupled-cluster [CCSD(T)] approximations, using large-core pseudopotential for Br atoms and the aug-cc-pV5Z basis set for He. The surface is characterized by three minima and the minimum energy pathways through them. The global minimum corresponds to a linear $He–Br_2–He$ configuration, while the two other ones to ''police-nightstick'' and tetrahedral structures. The corresponding well depths are $-90.39/-89.18$, $-81.23/-80.78$ and $-74.40/-74.02\ cm^{-1}$, respectively, at MP4/CCSD(T) levels of theory. It is found that results obtained by summing three-body parametrized $HeBr_2$ interactions and the He–He interaction are in very good accord with the corresponding MP4/CSSD(T) configuration energies of the He_2Br_2. Variational calculations using a sum of three-body interactions are presented to study the bound states of the vdW He_2Br_2 complex. The binding energy D_0 and the corresponding vibrationally averaged structure are determined for different isomers of the cluster and their comparison with the available experimental data is discussed. © *2005 American Institute of Physics.* [DOI: 10.1063/1.1833352]

I. INTRODUCTION

van der Waals (vdW) complexes of dihalogen molecule surrounded by several rare gas atoms have been intensely studied over the past decades by high resolution spectroscopy techniques. Such experimental investigations have covered a large number of vdW complexes including He_nI_n ($n=1-3$),[1] Ne_nI_2 ($n=1-6$),[2,3] Ne_nBr_2,[4] Rg_2Cl_2 (Rg = He,Ne,Ar)[5–7] and Ar_nHX (X = Cl or F and $n=1-3$ or 4).[8–10] The objective of these studies has been to elucidate the structure, spectroscopy and dynamics of vdW complexes and thus provide direct information on intermolecular forces.

An interesting example is the experimental studies by Janda and co-workers[5–7] on Rg_2Cl_2 clusters. Their attempt[5] to characterize the structure of the He_2Cl_2 complex has failed in fitting the rotationally resolved excitation spectrum using a rigid rotor tetrahedral structural model, which results in the formation pairwise additive potentials. Such structure has been successful in the cases of Ne_2Cl_2 and Ar_2Cl_2. Several similar rigid rotor geometries have also failed to fit their observed data. This led them to conclude that He_2Cl_2 is an extremely floppy, liquidlike cluster without any average structure and the dynamics of He_nCl_2 complexes will be quite different from their Rg_nCl_2 analogs. In situations like these, theoretical calculations on energetics and dynamics of such systems become indispensable for the quantitative modeling and interpretation of the experimental spectra.[11–16] Several theoretical studies based on a sum of atom-atom pairwise interactions and using quantum Monte Carlo[15] or variational[16] calculations have been carried out. Both results, in agreement with the experimental analysis, suggest the floppiness of the ground vdW state of He_nCl_2 ($n=2,3$) and emphasize the importance of performing exact calculations for such liquidlike systems.

Until recently, most models of vdW interactions were based on additive atom-atom forces. However, during the last few years *ab initio* methods have progressed sufficiently and interaction potentials between rare-gas atoms and a dihalogen molecule have been computed with high accuracy,[17,18] predicting the existence of two minima on the potential energy surface at linear and T-shaped configurations. A linear structure is not consistent with an additive pair potential form used for describing the intermolecular forces, and it became clear that even in the well region of a vdW bond such models do not work.[17,18] Linear species have been determined by microwave spectroscopy for several interhalogen complexes (Ar–ClF,[19] Kr–ClF,[20] He–ClF,[17] Ar–ICl[21]) and for $Ar–Cl_2$[22] and $Ar–I_2$.[23] Also, recent *ab initio* calculations confirm the existence of two isomers for $Rg–F_2$,[24] $Rg–Cl_2$,[25] $Rg–Br_2$,[26] and $Ar–I_2$[27] in accord with available experimental data.

Studies of larger species are more complex and the difficulty in the evaluation of their potential surfaces increases with their size. Up to now accurate potentials have been obtained by inversion of spectroscopic data[28,29] or through high level *ab initio* calculations[30–37] for several triatomic vdW systems. Thus, the interactions for such clusters are available with satisfactory accuracy, which permits the testing of various models of nonadditivity for their ability to reproduce a number of experimental observations. These facts made complexes composed of two rare-gas atoms and a dihalogen molecule especially attractive targets for the study of nonadditive forces. The first attempt to extract information on nonadditive interactions from spectroscopic data has been

[a]Author to whom correspondence should be addressed. Electronic mail: rita@imaff.cfmac.csic.es

undertaken by Hutson *et al.*[38] in similar vdW systems. They have used the microwave spectroscopic data of Klots *et al.*[39] to calculate a number of spectroscopic constants of the Ar_2HCl cluster, concluding that the data from the microwave spectra were not sufficient to reconstruct the three-body potential uniquely and more extensive regions of the potential surface should be measured. *Ab initio* studies have been also carried out[40,41] and the three-body effects in the Ar_2HF and Ar_2HCl clusters have been studied using Møller–Plesset pertubation theory, where the nonadditive interactions have been found to be large and repulsive around the equilibrium geometries for both systems. Later, Hutson and co-workers presented nonadditive potentials for Ar_2HF[42] and Ar_2HCl[43] incorporating different contributions to the three-body forces arising from the interaction between the permanent multipoles of the HF molecule and the exchange quadrupole caused by distortion of the two Ar atoms as they overlap.

The aim of the present study is to investigate the validity of the pairwise additivity of two- and three-body potentials for He_2Br_2. These results are compared with *ab initio* calculations and available experimental data and a simple model of the three-body potential is proposed to determine well depths and equilibrium structures for different isomeric configurations of the complex, as well as the minimum energy pathways through them. Additionally, variational methods are used to calculate the vibrational states of He_2Br_2. The wavefunctions of the lower states are analyzed in terms of probability distributions of the internal coordinates and the zero-point energy of the vdW cluster is evaluated. The paper is organized as follows. In the next section, together with the *ab initio* results, we compare results obtained using additive two- and three-body potentials. Bound state calculations using the sum of the three-body model surface are then reported and discussed in terms of available experimental data for similar systems. Conclusions constitute the closing section.

II. RESULTS

A. *Ab initio* calculations

The *ab initio* calculations are performed using the GAUSSIAN 98 package.[44] Computations are carried out at the MP4 and CCSD(T) levels of theory. The He_2-Br_2 system is described using the $(r,R_1,R_2,\theta_1,\theta_2,\gamma)$ coordinate system. r is the bond length of Br_2; R_1, R_2 are the intermolecular distances of each He atom from the center of mass of Br–Br, θ_1 is the angle between the $\mathbf{R}_1$ and $\mathbf{r}$ vectors, while θ_2 is the one between $\mathbf{R}_2$ and $\mathbf{r}$, and γ is the angle between the $\mathbf{R}_1$ and $\mathbf{R}_2$ vectors (see Fig. 1).

For the present calculation we used for Br atoms the Stuttgart–Dresden–Bonn (SDB) large-core energy-consistent pseudopotential[45] in conjunction with the augmented correlation consistent triple zeta (SDB-aug-cc-pVTZ) valence basis set.[46] This basis set is of cc-pVTZ quality and has been optimized for use with the SDB pseudopotential. For the He atoms we employed different basis sets such as the aug-cc-pV5Z and d-aug-cc-pV5Z from EMSL library.[47] Some convergence problems arose from the use of the double augmented basis sets imposing the use of the single augmented ones. In addition, the role of using bond functions, such as the $(3s3p2d2\,f1g)$ ones[48] is investigated. Test runs are carried out for a few specific configurationsi, as their location is not clearly defined, in the case of a polyatomic system. For example, choosing a tetrahedral structure of He_2Br_2, we present in Table I MP4 and CCSD(T) calculations for different intermolecular distances with and without the use of bond functions. A set of the $(3s3p2d2\,f1g)$ bond functions is located in the middle of the intermolecular distance R, which connects the centers of mass of He_2 and Br_2 molecules. As can be seen, the differences in the interaction energies obtained at both levels of theory are similar. It was found that their efficiency to saturate the dispersion energy accounts for an improvement of about 10%, around the equilibrium geometry. The effect of the use of bond functions has been found to be $\approx 5\%$ in other studies on triatomic dispersion-bound complexes.[49,50] Although, as the effect of their location for other configurations is still ambiguous, we choose to use for the He atoms the augmented correlation consistent (aug-cc-pV5Z) basis sets without the additional set of bond functions. In all calculations here $6d$ and $10f$ Cartesian functions are used.

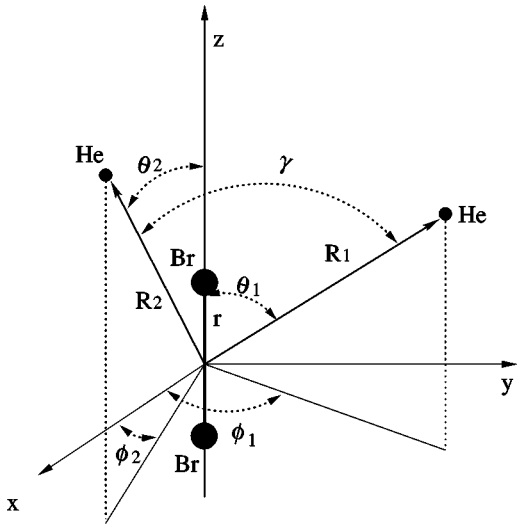

FIG. 1. Schematic representation of coordinate system for He_2Br_2 complex.

The supermolecular approach is used for the determination of the intermolecular energies, ΔE:

$$\Delta E = E_{He_2Br_2} - E_{BSSE} - E_{He_2} - E_{Br_2}, \quad (1)$$

TABLE I. MP4/CCSD(T) interaction energies of He_2Br_2 obtained with and without bond functons at the indicated tetrahedral configurations. bf stands for the $3s3p2d2\,f1g$ set of bond functions.

Method/R	3.0	3.25	3.5
MP4	−53.13	−72.86	−68.41
MP4+bf	−66.17	−81.78	−74.40
CCSD(T)	−53.57	−73.24	−68.59
CCSD(T)+bf	−66.48	−82.15	−74.56

TABLE II. MP4 interaction energies, ΔE [Eq. (1)] and ΔE^*, for the He_2Br_2 molecule for different structures and at the indicated coordinate values with r fixed at 2.281 Å (see Fig. 2). ΔE^* is calculated by $\Delta E^* = E_{He_2Br_2} - E_{BSSE^*} - E_{He} - E_{HeBr_2}$. Energy is in cm^{-1} and distances in Å.

Linear				Police-nightstick				Tetrahedral	
$R_1=R_2$	ΔE	$R_{1,2}$	ΔE^*	R_1	ΔE^*	R_2	ΔE^*	R	ΔE
4.3	−83.14	3.8	173.89	4.0	21.11	3.1	23.29	2.5	246.62
4.4	−89.77	3.9	79.91	4.1	−13.39	3.2	−4.28	2.6	135.37
4.5	−89.13	4.0	21.71	4.2	−32.53	3.3	−20.87	2.7	57.28
4.7	−77.72	4.1	−12.91	4.3	−41.88	3.4	−30.24	2.75	27.98
4.8	−70.23	4.2	−32.15	4.4	−45.15	3.5	−34.83	2.8	3.95
4.9	−62.68	4.3	−41.55	4.5	−44.79	3.6	−36.30	2.9	−31.19
5.0	−55.21	4.4	−44.86	4.7	−39.07	3.7	−35.80	3.0	−53.13
5.2	−42.78	4.5	−44.55	4.9	−31.49	3.9	−31.76	3.25	−72.87
5.5	−28.88	4.6	−42.20	5.2	−21.57	4.1	−26.42	3.5	−68.41
6.0	−15.25	4.7	−38.87	5.5	−14.55	4.3	−21.29	3.75	−56.56
6.5	−8.49	4.9	−31.34	6.0	−7.70	4.5	−16.94	4.0	−44.16
7.0	−4.96	5.2	−21.46	7.0	−2.55	5.0	−9.39	4.25	−33.67
8.0	−1.98	5.5	−14.46	9.0	−0.44	6.0	−3.12	4.5	−25.39
		6.0	−7.62			7.0	−1.23	4.75	−19.14
		7.0	−2.52			9.0	−0.29	5.0	−14.53
		9.0	−0.44					5.5	−8.52
								6.0	−5.20
								6.5	−3.29
								7.0	−2.13

where $E_{He_2Br_2}$, E_{He_2}, and E_{Br_2} are the energies of He_2-Br_2, He_2 and Br_2, respectively. The correction, (E_{BSSE}) for the basis-set superposition error is calculated using the standard counterpoise method.[51]

We performed MP4/CCSD(T) calculations for several configurations fixing the Br_2 bondlength at its equilibrium value $r_e=2.281$ Å. The results for the MP4 interaction energies at selected geometries are listed in Table II, while the optimal geometries and MP4/CCSD(T) energies for the three structures are shown in Fig. 2. The linear configuration has the lowest energy, $-90.39/-89.18\ cm^{-1}$ at MP4/CCSD(T) levels with $R_1=R_2=4.44$ Å. The next two equlibrium structures are found at energies of $-81.23/-80.78\ cm^{-1}$ and $-74.40/-74.02\ cm^{-1}$, respectively, and correspond to a "police–nightstick" ($R_1=4.44$ Å and $R_2=3.58$ Å) and tetrahedral ($R=3.33$ Å) configurations. We should note that the equilibrium distances of the above structures are very close to the ones obtained by CCSD(T) calculations for the optimized linear and T-shaped geometries for the triatomic $HeBr_2$ complex.[52]

In order to extract information on nonadditive interactions in He_2Br_2 we examine the above equilibrium structures based on the *ab initio* calculations and partitioning the interaction energy into components, as given in Ref. 41. Therefore, we show in Table III the summary of supermolecular calculations of the entire nonadditivity in the three He_2Br_2 equilibrium structures using the results of the MPPT (Møller–Plesset perturbation theory) up to fourth order along with the ones of the CCSD(T) method. As can be seen in Table III, the total three-body interaction for the three different equlibrium geometries computed through the MP3 amounts to -77.76, -70.06 and $-62.88\ cm^{-1}$, respectively. These energies neglect completely the effects of intramonomer correlation on three-body dispersion. The major effect of the intrasystem correlation on dispersion appears in the MP4 level and is especially sensitive to the presence of triple excitations. For all configurations studied the MP4(SDQ) level reduces this effect to -71.29, -65.35 and $-59.09\ cm^{-1}$, respectively, while the inclusion of triples enhances both MP4(SDQ) and CCSD interaction energies [see MP4(SDTQ) and CCSD(T) values in Table III]. The MP4(SDQ) results seem to be well converged with respect to

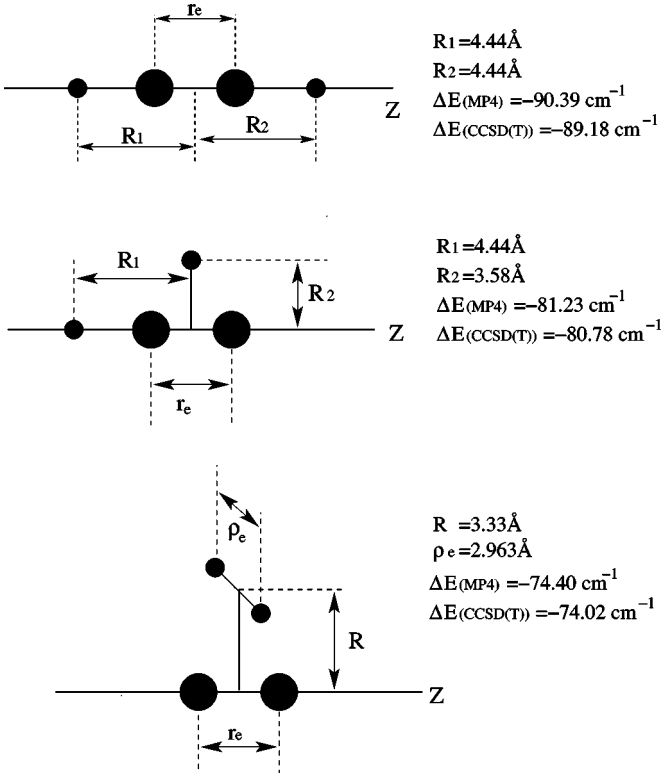

FIG. 2. Optimal MP4/CCSD(T) structures for He_2Br_2.

TABLE III. Summary of the supermolecular calculations of the nonadditive effects around the three equilibrium He_2Br_2 structures. Energy is in cm^{-1} and distances in Å.

$R_{1,2}$/Method	HF	MP2	MP3	MP4(SDQ)	MP4(SDTQ)	CCSD	CCSD(T)
			Linear structure				
4.3	125.57	−75.57	−69.09	−61.26	−83.14	−59.87	−81.67
4.4	84.41	−83.42	−77.76	−71.29	−89.77	−70.23	−88.49
4.5	56.45	−83.91	−78.88	−73.50	−89.15	−72.69	−88.01
			Police-nightstick structure				
$R_{1,2}$/Method	HF	MP2	MP3	MP4(SDQ)	MP4(SDTQ)	CCSD	CCSD(T)
4.3	97.10	−70.21	−65.76	−60.38	−77.67	−59.41	−77.06
4.4	76.49	−74.12	−70.06	−65.36	−80.94	−64.57	−80.44
4.5	62.53	−74.34	−70.58	−66.48	−80.59	−65.80	−80.20
			Tetrahedral structure				
R/Method	HF	MP2	MP3	MP4(SDQ)	MP4(SDTQ)	CCSD	CCSD(T)
3.0	154.18	−42.58	−39.53	−35.31	−53.14	−34.26	−53.57
3.25	70.80	−65.71	−62.88	−59.94	−72.87	−59.43	−73.24
3.5	31.87	−63.58	−61.06	−58.10	−68.41	−58.69	−68.59

the CCSD calculations, For a consistent treatment of two- and three-body correlation effects, the three-body potentials should be summed to a level one order higher than the corresponding two-body ones. The MP4(SDTQ) reproduces quantitatively the dominant contributions to the two-body interaction energy, while to achieve a similar level of correlation for the three-body terms one needs to advance to next order of theory, practically more accurate to turn to the CCSD(T) theory. Our calculations indicate that the total nonadditive effect in He_2Br_2 originating from supermolecular CCSD(T) calculations amounts to -88.49, -80.44 and $-73.24\,cm^{-1}$ for configurations nearby its equilibrium structures. We should mention that the same behavior were observed in the results of the MPPT energies for the $HeBr_2$ complex[52] around its linear and T-shaped equilibrium configurations. This finding indicates a similar nature of binding in triatomic and tetratomic complexes of such type, and thus information on intermolecular interactions available for triatomic species might serve to study larger systems.

B. Analytical representation of the PESs

Two functional forms are checked for the He_2-Br_2 potential energy function. One is based on the pairwise atom-atom interaction, which has been widely used in all previous calculations on triatomic and tetratomic, Rg_n-X_2 with $n=1,2$, complexes.[15,16,53–55] The parameters for the two-body interactions are taken from Ref. 56. The second one is given by summing up three-body $HeBr_2$ interactions and the He–He one,

$$V(r_e,R_1,R_2,\theta_1,\theta_2,\gamma) = \sum_i V_{\mathrm{He}_i\mathrm{Br}_2}(r_e,R_i,\theta_i) + V_{\mathrm{HeHe}}(R_1,R_2,\gamma), \qquad (2)$$

where the corresponding $V_{\mathrm{He}_i\mathrm{Br}_2}(r_e,R_i,\theta_i)$ terms with $i=1$ and 2 are the CCSD(T) parametrized potential of the $HeBr_2$ complex[52] and $V_{\mathrm{HeHe}}(R_1,R_2,\gamma)$ term is the potential function for He_2 given in Ref. 57.

Configuration energies are determined by optimizing different structures with respect to atomic positions using the above mentioned functional expressions. In Fig. 3 we compare the two different potential functional forms with the

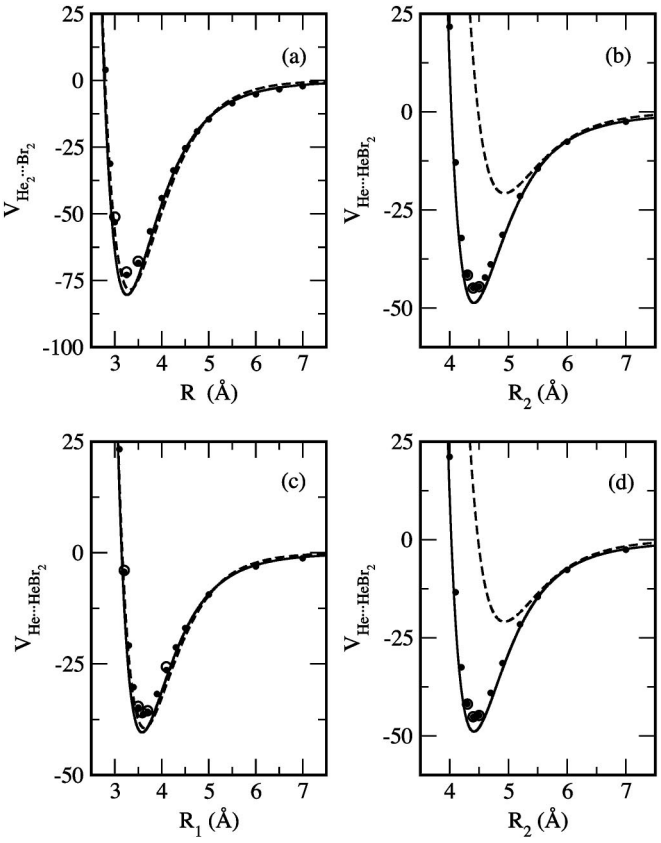

FIG. 3. Comparison of two different potential energy curves for tetrahedron (a), linear (b) and police-nightstick (c), (d) orientations of He_2Br_2. Solid lines are for the sum of three-body CCSD(T) interaction potential, while dotted lines correspond to the pairwise atom-atom form. The MP4 *ab initio* values are also indicated by filled circles, whereas potential values obtained using the sum of three-body MP4 interaction $HeBr_2$ potential are shown by open circles.

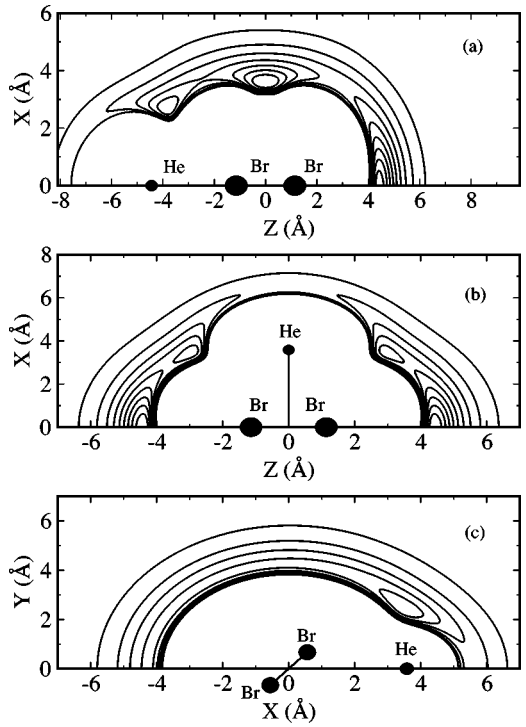

FIG. 4. Contour plots of the He_2Br_2 potential energy surface, $V(r_e, R_1, R_2, \theta_1, \theta_2, \gamma)$, Eq. (2) in the XY (a), (b) or ZX (c) plane. The Br_2 distance is fixed at 2.281 Å along the Z-axis, while the geometry of the triatomic molecule is fixed to a linear configuration with $R_1 = 4.87$ Å (a), and to a T-shaped configuration with $R_1 = 3.59$ Å [(b) and (c)]. Contour intervals are of 5 cm^{-1} and for energies from -80 to -40 cm^{-1} (a), -85 to -40 cm^{-1} (b), and -65 to -40 cm^{-1} (c).

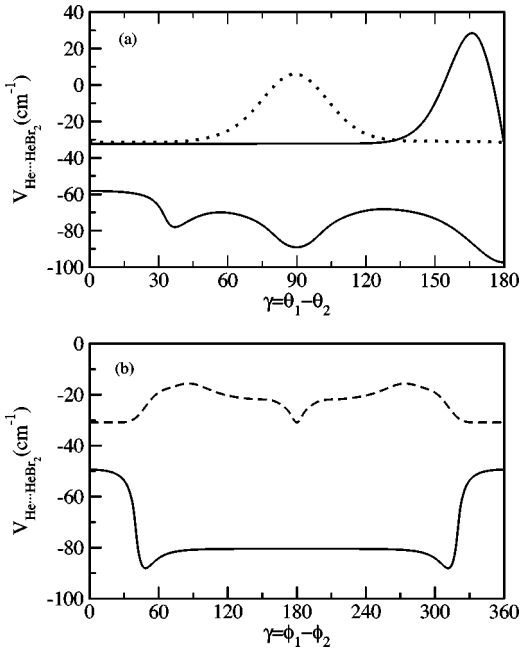

FIG. 5. Minimum energy path, V_m in cm^{-1} as a function of angle γ, for planar $\gamma = (\theta_1 - \theta_2)$ (a) and no-planar with $\theta_1 = \theta_2 = 90°$, $\gamma = (\phi_1 - \phi_2)$ with $\theta_1 = \theta_2 = 90°$ (b) configurations. The probability $\int |\Psi|^2 \sin\gamma dR$ distributions for $n = 0$(collinear), $n = 1$(police-nightstick) and $n = 2$(tetrahedral) vdW levels of He_2Br_2 are also depicted.

MP4 *ab initio* results. Solid lines are for the sum of the three-body CCSD(T) $HeBr_2$ interaction potential, dashed lines correspond to the pairwise atom-atom form, while filled circles indicate the MP4 *ab initio* values. Open circles are for the potential values obtained using the sum of the three-body MP4 potential for $HeBr_2$, at the specific geometries with the same basis set as in the He_2Br_2 calculations. Figure 3(a) represents the potential energy curves as a function of the distance R between the center of masses of Br_2 and He_2 in the tetrahedron structure. As can be seen, both forms represent well the *ab initio* data at this configuration. In Fig. 3(b) a one-dimensional plot for the linear geometry is shown. The interaction potential is plotted as a function of R_2 distance (see Fig. 2), while in Figs. 3(c) and 3(d) representations of the potential energy are given for the ''police-nightstick'' structure as a function of R_1 and R_2 distances, respectively. The additive atom-atom interactions form predicts the overall minimum of the well for a distorted tetrahedron, while the sum of the three-body $HeBr_2$ interactions evaluates a linear structure as the global minimum, and two other ones, ''police-nightstick'' and tetrahedral, as local minima of the He_2Br_2 surface. As can be seen, results obtained using the sum of the three-body $HeBr_2$ interactions are in very good accord with the corresponding *ab initio* values. Contrarily, large deviations from the *ab initio* results are found to the values predicted by the pairwise atom-atom interactions form, particularly for linear configurations. Thus, we choose the sum of the three-body CCSD(T) $HeBr_2$ interactions henceforth to represent the potential surface of He_2Br_2 and to check further its validity in comparison with *ab initio* data.

Figure 4 shows two-dimensional contour plots of the $V(r_e, R_1, R_2, \theta_1, \theta_2, \gamma)$ surface in the XY or ZX Cartesian plane. The equipotential curves are shown for He moving around a triatomic $HeBr_2$ molecule fixed at specific linear [see Fig. 4(a)] and T-shaped [see Fig. 4(b) and 4(c) configurations. The potential has three wells at energies of -97.39, -88.88 and -80.38 cm^{-1}, with the collinear well to be the deeper than the ''police-nightstick'' and tetrahedral ones. The equilibrium distances and angles are at $R_1^e = R_2^e = 4.41$ Å for the linear well, $R_1^e = 4.41$, $R_2^e = 3.58$ Å for the ''police-nightstick'' one and $R^e = 3.27$ Å for the tetrahedral well. The isomerization barrier between the collinear↔police-nightstick wells is found at energy of -68.15 cm^{-1} and an angle of 127°. One-dimensional representations of the potential are shown in Fig. 5, where minimum energy paths are plotted as a function of the angle $\gamma = \theta_1 - \theta_2$ for planar [see Fig. 5(a)] and no-planar with $\theta_1 = \theta_2 = 90°$ and $\gamma = \phi_1 - \phi_2$ [see Fig. 5(b)] configurations.

In Table IV we present for the indicated geometries, selected along a minimum energy path ($HeBr_2$ molecule is fixed at linear configuration, $\theta_1 = 180$ [see Fig. 2(a)], while the R_1 and R_2 distances are optimized for each θ_2 value), the *ab initio* MP4 and CCSD(T) values and compare them with the corresponding $V(r_e, R_1, R_2, \theta_1, \theta_2, \gamma)$ ones, given by Eq. (2). For the sake of comparison the potential values using the two-body potential form are also listed in the last column. As can be seen, the differences obtained in the CCSD(T) results are fully justified due to the different basis sets used, including or not bond functions, in the *ab initio* calculations of the triatomic and tetratomic complexes, respectively. We should

TABLE IV. MP4/CCSD(T) interaction energies, ΔE [Eq. (1)] and potential values obtained from Eq. (2) using three-body (3B) MP4, CCSD(T) and CCSD(T)+bf $HeBr_2$ interaction potentials for the He_2-Br_2 complex at the indicated (θ_2, R_1, R_2) points. The potential values based on the two-body (2B) sum are also listed. Energies in cm^{-1}, angles in degrees and distances in Å.

(θ_2, R_1, R_2)	MP4/CCSD(T)	$V_{3B(MP4)}/V_{3B(CCSD(T))}/V_{3B(CCSD(T)+bf)}$	V_{2B}
(0,4.41,4.41)	−90.01/−88.80	−90.03/−88.71/−97.39	22.11
(15,4.41,4.52)	−78.95/−77.87	−78.95/−77.80/−85.67	1.45
(30,4.41,4.65)	−67.36/−66.48	−67.33/−66.41/−73.32	−10.10
(45,4.41,4.60)	−63.06/−62.29	−63.03/−62.26/−68.69	−11.23
(60,4.41,4.34)	−63.01/−62.62	−62.99/−62.57/−68.97	−13.83
(75,4.41,3.92)	−69.99/−69.40	−69.95/−69.35/−76.38	−21.81
(90,4.41,3.58)	−81.03/−80.59	−80.96/−80.46/−88.88	−27.95
(105,4.41,3.92)	−69.99/−69.51	−69.95/−69.35/−76.38	−21.82
(120,4.41,4.33)	−63.19/−62.57	−63.21/−62.53/−68.96	−13.99
(135,4.41,4.57)	−64.04/−62.29	−62.90/−62.16/−68.65	−11.49
(150,4.40,5.48)	−56.54/−55.77	−56.34/−55.68/−60.54	1.72
(165,4.40,6.92)	−47.82/−47.03	−47.49/−46.92/−52.94	11.39
(180,4.41,7.34)	−47.01/−46.33	−46.79/−46.11/−50.43	10.08

note that CCSD(T) results are within the difference of 10% in the interaction energies attributed from the test runs to the use of bond functions (see Table I).

C. Bound state calculations

The Hamiltonian operator in the coordinate system shown in Fig. 1 has the form[16,58]

$$\hat{H} = -\frac{\hbar^2}{2\mu_1}\left(\frac{\partial^2}{\partial R_1^2} + \frac{2}{R_1}\frac{\partial}{\partial R_1}\right) - \frac{\hbar^2}{2\mu_2}\left(\frac{\partial^2}{\partial R_2^2} + \frac{2}{R_2}\frac{\partial}{\partial R_2}\right) + \frac{\hat{j}^2}{2\mu_3 r_e^2} + \frac{\hat{l}_1^2}{2\mu_1 R_1^2} + \frac{\hat{l}_2^2}{2\mu_2 R_2^2} - \frac{\hbar^2}{2m_{\mathrm{Br}}}\nabla_1\cdot\nabla_2 + V(\mathbf{r},\mathbf{R}_1,\mathbf{R}_2), \quad (3)$$

where $\mu_1^{-1} = \mu_2^{-1} = m_{\mathrm{He}}^{-1} + (m_{\mathrm{Br}} + m_{\mathrm{Br}})^{-1}$ and $\mu_3^{-1} = m_{\mathrm{Br}}^{-1} + m_{\mathrm{Br}}^{-1}$ are the reduced masses, $m_{\mathrm{He}} = 4.0026$ amu and $m_{\mathrm{Br}} = 78.918\,336\,1$ amu are the atomic masses of ^{4}He and ^{79}Br isotopes, and $\hat{l}_1$, $\hat{l}_2$ and $\hat{j}$ are the angular momenta associated with the vectors $\mathbf{R}_1$ $\mathbf{R}_2$ and $\mathbf{r}$, respectively, leading to a total angular momentum $\hat{J} = \hat{l}_1 + \hat{l}_2 + \hat{j} = \hat{L} + \hat{j}$. r is fixed at the equilibrium Br–Br bond length (r_e), and the potential for He_2Br_2 complex is given by the expansion in Eq. (2).

For a total angular momentum J, the Hamiltonian of Eq. (3) is represented in a set of basis functions consisting of linear combinations of products of bidimensional radial functions by angular functions, which incorporate the whole symmetry of the system.[16] For the R_1 and R_2 coordinates numerical $\{\xi_n(R_i)\}$, with $i=1,2$ and $n=1,\ldots,N_R$ functions are used. We evaluate them as follows: First, the two-dimensional Schrödinger equation is solved in (R,θ,r_e) variables for a triatomic He–Br_2 system at total angular momentum zero. The employed PES was the CCSD(T) *ab initio* surface given in Ref. 52, and a discrete variable representation (DVR) basis seti[59] is used. It consists of functions given by $f_l(R) = [2/\sqrt{\mathcal{L}(N+1)}]\,\Sigma_{k=1}^{N}\sin[k\pi(R - R^{\min})/\mathcal{L}]\sin[k\pi l/(N+1)]$ where N is the total number of DVR points, $\mathcal{L}$ is $R_i^{\max} - R_i^{\min}$, and the DVR points in the R coordinate are $R^l = l\mathcal{L}/(N+1) + R^{\min}$ for $l=1,\ldots,N$. Second, considering a set of the N_R lowest eigenstates, their corresponding radial distributions are orthonormalized through a Gram–Schmidt procedure, and constitute the radial basis set, $\{\xi_n(R_i)\}$, for the tetraatomic calculations.

TABLE V. Binding energies (D_0) and vibrationally averaged structures $(R_{1,2}^0)$ for the three He_2Br_2 isomers. Energies in cm^{-1} and distances in Å.

Configuration	D_0 (cm^{-1})	$R_{1,2}^0$ (Å)
Linear	32.240	4.867
Police-nightstick	31.437	4.491
Tetrahedral	30.930	4.171

For the angular basis functions, we consider the following linear combinations, which are eigenfunctions of the parity of total nuclear coordinates inversion p:

$$\mathcal{F}_{l_1 l_2 L|\Omega|}^{(JMp)} = \sqrt{\frac{1}{2(1+\delta_{|\Omega|0})}}\left[\mathcal{W}_{l_1 l_2 L\Omega}^{(JM)} + p(-1)^{J+l_1+l_2+L}\mathcal{W}_{l_1 l_2 L-\Omega}^{(JM)}\right] \quad (4)$$

with

$$\mathcal{W}_{l_1 l_2 L\Omega}^{(JM)} = \sqrt{\frac{2J+1}{4\pi}}\mathcal{D}_{M\Omega}^{J*}(\phi_r,\theta_r,0)\mathcal{Y}_{l_1 l_2}^{L\Omega}(\mathbf{R}_1,\mathbf{R}_2), \quad (5)$$

M is the projection of J on the space-fixed z-axis and Ω is its projection on the body-fixed z-axis, which is chosen here along the $\mathbf{r}$ vector. The $\mathcal{D}_{M\Omega}^{J}$ are Wigner matrices[60] and $\mathcal{Y}_{l_1 l_2}^{L\Omega}$ are angular functions[61] in the coupled BF representation.

In turn, taking into account that in the case of He_2Br_2 the Hamiltonian is also invariant under $\mathbf{R}_1 \leftrightarrow \mathbf{R}_2$ inversion, then a well-defined parity, p_{12}, basis set is built up as follows:

$$\Phi_{l_1 l_2 L|\Omega|nm}^{JMpp_{12}} = \sqrt{\frac{1}{2(1+\delta_{nm}\delta_{l_1 l_2})}}\left[\Phi_{l_1 l_2 L|\Omega|nm}^{JMp} + p_{12}(-1)^{l_1+l_2+L}\Phi_{l_1 l_2 L|\Omega|mn}^{JMp}\right], \quad (6)$$

where $\Phi_{l_1 l_2 L|\Omega|nm}^{JMp} = \phi_{nm}\mathcal{F}_{l_1 l_2 L|\Omega|}^{(JMp)}$ and $\phi_{nm}(R_1,R_2) = \xi_n(R_1)\xi_m(R_2)/R_1R_2$.

For the evaluation of the Hamiltonian matrix elements, the numerical set of the radial basis functions $\{\xi_n(R_i)\}$ mentioned above, is represented as linear combinations of the f_l DVR functions, $\xi_n(R_i) = \Sigma_{l=1}^{N}(\xi_n|f_l\rangle f_l(R_i) = \Sigma\xi_n(R_i^l)f_l(R_i)$, $i=1,2$ and $n=1,\ldots,N_R$. The matrix elements of the Hamiltonian are given in Ref. 16.

In our calculations at $J=0$, $N_R=7$ radial numerical functions, represented at 50 DVR points over the range of 2.5 to 8 Å, for each R_1 and R_2 coordinate are used. In turn, values of $L=j=0-12$ (even) with $l_1^{\max}=l_2^{\max}=12$ for even $[p_{12}=(-1)^{l_1+l_2+L}=+1]$ and $p=(-1)^{J+L+l_1+l_2}$ parity symmetries were enough to achieve convergence in the variational calculation.

The three lowest vibrational states of He_2Br_2 are found at energies of -32.240, -31.437 and $-30.930\,cm^{-1}$ (see Table V and Figs. 5 and 6). In Fig. 5, together with the minimum energy path, we plot the angular probability den-

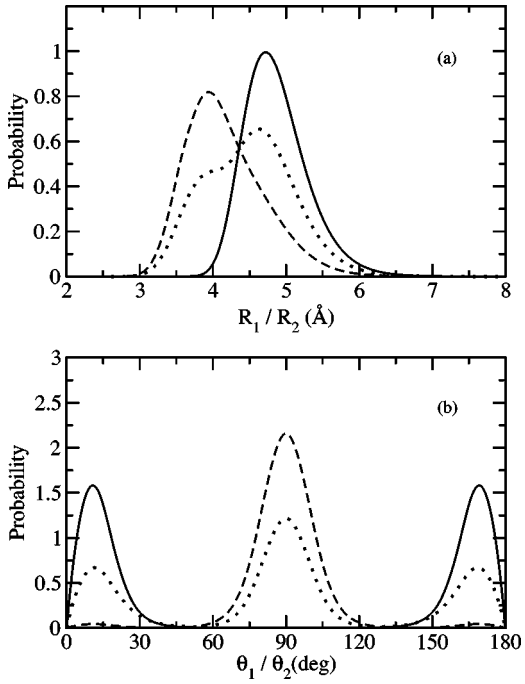

FIG. 6. Radial (a) and angular (b) probability densities for the indicated vdW levels of He_2Br_2 for $J=0$ calculated using the $V(r_e, R_1, R_2, \theta_1, \theta_2, \gamma)$ PES.

sity of the angle γ for the $n=0$ (solid line), $n=1$ (dotted line) [see Fig. 5(a)] and $n=2$ (dashed line) [see Fig. 5(b)] eigenfunctions, while in Fig. 6 the radial $R_{i=1,2}$ and angular $\theta_{i=1,2}$ distributions for these states are shown. As can be seen, $n=0$ state is localized in the linear well and its distributions show peak at $\theta_{1,2}=0{,}180°$, $R_{1,2}=4.722$ Å and $\gamma=180°$. The $n=1$ state corresponds to "police-nightstick" configurations, with two maxima at $\theta_{1,2}=90$ and 0/180°, and at $R_{1,2}=3.98$ and 4.631 Å, and only one peak at $\gamma=90°$ [see Fig. 5(a)], while the $n=2$ state exhibits a tetrahedral structure with a maximum value at $\theta_{1,2}=90°$ and $R_{1,2}=3.940$ Å and a broad distribution in γ, except a small peak at $\gamma \approx 60°$, where the He–He attractive interaction is maximum. There is a forbidden area around $\gamma=0$ where the two atoms are collided [see Fig. 5(b)]. The radial expectation values for each of the above structures, R_i^0, obtained by averaging R_i over the corresponding distributions, are listed in Table V. To our knowledge, for first time such results on the vibrationally averaged structures of He_2Br_2 are presented. In contrast with previous studies[5,15,16] on He_2Cl_2 cluster, in the present work localized structures are determined for the lower He_2Br_2 vdW states. Traditional models based on a He_2Cl_2 tetrahedron frozen stucture have failed to reproduce the experimental absorption spectrum, suggesting a quite delocalized structure for its vibrationally ground state.[5] Here, based on *ab initio* calculations, we propose different structural models, like linear or "police-nightstick," in order to fit the rotationally resolved excitation spectrum of He_2Cl_2 or similar species.

We should note that the energy difference between the above mentioned isomers is small, and the lack of the r dependence in the potential form might influence their relative stability. For the triatomic vdW complexes of He atom with homopolar/heteropolar halogens, it has been found[18,24,25,52] that the energy difference between the linear and T-shaped wells increases when the r bond is lengthened, and a similar behavior should be expected for the tetratomic complexes. However, in order to justify our assertions for such tetratomic species, comparison with experimental measurements is needed, which would finally contribute to evaluate the present CCSD(T) potential.

III. CONCLUSIONS

The ground potential energy surface is calculated for the He_2Br_2 complex, where the Br_2 molecule is frozen at its equilibrium bondlength, at the MP4/CCSD(T) level of theory. Analytical representations based on a sum of pairwise atom-atom interactions and a sum of three-body $HeBr_2$ CCSD(T) potentials and He–He interaction are checked in comparison with the tetratomic *ab initio* results. The sum of the three-body interactions form is found to be able to accurately represent the MP4/CCSD(T) data. For the first time an analytical expression in accord with high level *ab initio* studies is proposed for describing the intermolecular interactions for such two- atom rare-gas–dihalogen complexes. The existence of three (linear, "police-nightstick" and tetrahedral) minima is established for the He_2Br_2 ground PES. This finding may contribute to fit the rotationally resolved excitation spectrum of He_2Cl_2 or similar species, where the traditional tetrahedral structural models, based on pairwise additive potentials, have failed.

Variational bound state calculation is carried out for the above surface and vdW energy levels and eigenfunctions for $J=0$ are evaluated for He_2Br_2. Radial and angular distributions are calculated for the three lower vdW states. All of them are well localized in configuration space, with an exception of the broad distribution of the angle γ for the $n=2$ state, due to the weak He–He interaction. The ground state corresponds to a linear isomer and the next two excited vdW levels are assigned to "police-nightstick" and tetrahedral ones. The binding energies and the average structures for these species are determined to be $D_0=32.240\ \mathrm{cm}^{-1}$ with $R_{1,2}^0=4.867$ Å, $D_0=31.437\ \mathrm{cm}^{-1}$ with $R_{1,2}^0=4.491$ Å, and $D_0=30.930\ \mathrm{cm}^{-1}$ with $R_{1,2}^0=4.171$ Å, respectively.

Whether the properties of the weak bonding in such systems can be predicted by the sum of atom-diatom interactions deserve further investigation. Such model should be applicable to a broad class of Rg_2XY, with Rg=rare gas and X,Y=halogen atoms, vdW clusters. It is particularly interesting to investigate the intermolecular interactions and structural properties of similar clusters consisting of heteropolar halogens, evaluating the importance of additional effects (e.g., introducing electric dipole moment, changing the reduced mass of the complex, etc.). Work in this line is in progress.

ACKNOWLEDGMENTS

The authors wish to thank the Centro de Calculo de IMAFF, the Centro Técnico de Informática (CTI), CSIC, the Centro de Supercomputación de Galicia (CESGA) and the Grupo de SuperComputación del CIEMAT (GSC) for alloca-

tion of computer time. This work has been supported by CICYT, Spain, Grant No. BFM 2001-2179 and by a European TMR network, Grant No. HPRN-CT-1999-00005. R.P. acknowledges a contract from the Comunidad Autónoma de Madrid, Spain.

[1] W. Sharfin, K. E. Johnson, L. Wharton, and D. H. Levy, J. Chem. Phys. **71**, 1292 (1979).
[2] J. E. Kenny, K. E. Johnson, W. Sharfin, and D. H. Levy, J. Chem. Phys. **72**, 1109 (1980).
[3] M. Gutmann, D. M. Willberg, and A. H. Zewail, J. Chem. Phys. **97**, 8048 (1992).
[4] B. A. Swartz, D. E. Brinza, C. M. Western, and K. C. Janda, J. Phys. Chem. **88**, 6272 (1984).
[5] W. D. Sands, C. R. Bieler, and K. C. Janda, J. Chem. Phys. **95**, 729 (1991).
[6] S. R. Hair, J. I. Cline, C. R. Bieler, and K. C. Janda, J. Chem. Phys. **90**, 2935 (1989).
[7] C. R. Bieler, D. D. Edvard, and K. C. Janda, J. Chem. Phys. **94**, 7452 (1990).
[8] H. S. Gutowsky, T. D. Klots, C. Chuang, J. D. Keen, C. A. Schmuttenmaer, and T. Emilsson, J. Am. Chem. Soc. **109**, 5653 (1987).
[9] A. McIlroy, R. Lascola, C. M. Lovejoy, and D. J. Nesbitt, J. Chem. Phys. **95**, 2636 (1991).
[10] M. J. Elrod, D. W. Steyert, and R. J. Saykally, J. Chem. Phys. **95**, 3182 (1991).
[11] P. Villarreal, A. Varadé, and G. Delgado-Barrio, J. Chem. Phys. **90**, 2684 (1989).
[12] P. Villarreal, S. Miret-Artés, O. Roncero, S. Serna, J. Campos-Martínez, and G. Delgado-Barrio, J. Chem. Phys. **93**, 4016 (1990).
[13] A. García-Vela, P. Villarreal, and G. Delgado-Barrio, J. Chem. Phys. **92**, 496 (1990).
[14] E. Le Quéré and S. K. Gray, J. Chem. Phys. **98**, 5396 (1993).
[15] Z. Bacic, M. Kennedy-Mandziuk, J. W. Moskowitz, and K. E. Schmidt, J. Chem. Phys. **97**, 6472 (1992).
[16] P. Villarreal, O. Roncero, and G. Delgado-Barrio, J. Chem. Phys. **101**, 2217 (1994).
[17] K. Higgins, F.-M. Tao, and W. Klemprerer, J. Chem. Phys. **109**, 3048 (1998).
[18] R. Prosmiti, C. Cunha, P. Villarreal, and G. Delgado-Barrio, J. Chem. Phys. **119**, 4216 (2003).
[19] S. J. Harris, S. E. Novick, W. Klemperer, and W. E. Falconer, J. Chem. Phys. **61**, 193 (1974).
[20] S. E. Novick, S. J. Harris, K. C. Janda, and W. Klemperer, Can. J. Phys. **53**, 2007 (1975).
[21] J. B. Davey, A. C. Legon, and E. R. Waclawicki, Chem. Phys. Lett. **306**, 133 (1999).
[22] Y. Xu, W. Jäger, I. Ozier, and M. C. L. Gerry, J. Chem. Phys. **98**, 3726 (1993).
[23] A. E. Stevens Miller, C.-C. Chuang, H. C. Fu, K. J. Higgins, and W. Klemperer, J. Chem. Phys. **111**, 7844 (1999).
[24] K. W. Chan, T. D. Power, J. Jai-nhuknan, and S. M. Cybulski, J. Chem. Phys. **110**, 860 (1999).
[25] S. M. Cybulski and J. S. Holt, J. Chem. Phys. **110**, 7745 (1999).
[26] R. Prosmiti, C. Cunha, P. Villarreal, and G. Delgado-Barrio, J. Chem. Phys. **116**, 9249 (2002).
[27] R. Prosmiti, P. Villarreal, and G. Delgado-Barrio, Chem. Phys. Lett. **359**, 473 (2002).
[28] J. M. Hutson, J. Chem. Phys. **96**, 6752 (1992).
[29] J. M. Hutson, J. Chem. Phys. **89**, 4550 (1988).
[30] S. M. Cybulski and J. S. Holt, J. Chem. Phys. **110**, 7745 (1999).
[31] F. Y. Naumikin, ChemPhysChem **2**, 121 (2001).
[32] G. Chalasinski and M. M. Szczesniak, Chem. Rev. **100**, 4227 (2000).
[33] A. Rohrbacher, J. Williams, K. C. Janda, S. M. Cybulski, R. Burcl, M. M. Szcześniak, G. Chalasiński, and N. Halberstadt, J. Chem. Phys. **106**, 2685 (1997).
[34] R. Prosmiti, C. Cunha, P. Villarreal, and G. Delgado-Barrio, J. Chem. Phys. **117**, 7017 (2002).
[35] A. Valdés, R. Prosmiti, P. Villarreal, and G. Delgado-Barrio, Chem. Phys. Lett. **357**, 328 (2003).
[36] R. Prosmiti, P. Villarreal, and G. Delgado-Barrio, Isr. J. Chem. **43**, 297 (2003).
[37] A. Valdés, R. Prosmiti, P. Villarreal, and G. Delgado-Barrio, J. Phys. Chem. A **108**, 6065 (2004).
[38] J. M. Hutson, J. A. Beswick, and N. Halberstadt, J. Chem. Phys. **90**, 1337 (1989).
[39] T. D. Klots, C. Chuang, R. S. Ruoff, T. Emilsson, and H. S. Gutowsky, J. Chem. Phys. **86**, 5315 (1987); **87**, 4383 (1987).
[40] G. Chalasinski, M. M. Szcześniak, and B. Kukawska-Tarnawska, J. Chem. Phys. **94**, 6677 (1991).
[41] M. M. Szcześniak, G. Chalasinski, and P. Piecuch, J. Chem. Phys. **99**, 6732 (1993).
[42] A. Ernesti and J. M. Hutson, Phys. Rev. A **51**, 239 (1995).
[43] A. R. Cooper and J. M. Hutson, J. Chem. Phys. **98**, 5337 (1993).
[44] GAUSSIAN 98, Revision A.7, M. J. Frisch, G. W. Trucks, H. B. Schlegel *et al.* (Gaussian, Inc., Pittsburgh, PA, 1998).
[45] A. Bergner, M. Dolg, W. Kuechle, H. Stoll, and H. Preuss, Mol. Phys. **80**, 1431 (1993).
[46] J. M. L. Martin and A. Sundermann, J. Chem. Phys. **114**, 3408 (2001).
[47] Enviromental Molecular Sciences Laboratory, http://www.emsl.pnl.gov/.
[48] S. M. Cybulski and R. R. Toczylowski, J. Chem. Phys. **111**, 10520 (1999).
[49] F.-M. Tao and W. Klemperer, J. Chem. Phys. **97**, 440 (1992).
[50] G. Chalasinski and M. M. Szczesniak, Chem. Rev. **94**, 1723 (1994).
[51] S. F. Boys and F. Bernardi, Mol. Phys. **19**, 553 (1970).
[52] A. Valdés, R. Prosmiti, P. Villarreal, and G. Delgado-Barrio, Mol. Phys. (to be published).
[53] M. I. Hernández, A. Garcia-Vela, J. Campos-Martnez, O. Roncero, P. Villarreal, and G. Delgado-Barrio, Comput. Phys. Commun. **145**, 97 (2002).
[54] A. Rohrbacher, J. Williams, and K. C. Janda, Phys. Chem. Chem. Phys. **1**, 5263 (1999).
[55] M. I. Hernández, T. González-Lezana, G. Delgado-Barrio, P. Villarreal, and A. A. Buchachenko, J. Chem. Phys. **113**, 4620 (2000).
[56] T. González-Lezana, M. I. Hernández, G. Delgado-Barrio, A. A. Buchachenko, and P. Villarreal, J. Chem. Phys. **105**, 7454 (1996).
[57] R. A. Aziz and M. J. Slaman, J. Chem. Phys. **94**, 8047 (1991).
[58] X. Chapuisat, A. Belafhal, and N. Nauts, J. Mol. Spectrosc. **149**, 274 (1991).
[59] J. T. Muckerman, Chem. Phys. Lett. **173**, 200 (1990).
[60] R. N. Zare, *Angular Momentum* (Wiley, New York, 1988).
[61] G. Danby, J. Phys. B **16**, 3393 (1983).